

Article

Research and Application of Deep Profile Control Technology in Narrow Fluvial Sand Bodies

Xu Zheng ¹, Yu Wang ¹, Yuan Lei ¹, Dong Zhang ^{1,*}, Wenbo Bao ¹ and Shijun Huang ²¹ Tianjin Branch of CNOOC Ltd., Tianjin 300459, China² Institute of Petroleum Engineering, China University of Petroleum (Beijing), Beijing 102249, China

* Correspondence: zhangdong18@cnooc.com.cn

Abstract: Narrow Fluvial Sand Bodies are primarily developed along the river center, with horizontal wells for injection and production in some Bohai waterflooded oilfields. This results in a rapid increase in water cut due to a single injection–production direction. Over time, dominant water breakthrough channels form between wells, and the remaining oil moves to deeper regions, which makes conventional profile control measures less effective. We developed a quantitative method based on integrated dynamic and static big data to identify these breakthrough channels and measure the flow intensity between injection and production wells. To address deep remaining oil mobilization, we performed micro-analysis and physical simulations with heterogeneous core models, which led to the development of a deep profile control system using emulsion polymer gel and self-assembling particle flooding. Experiments show that the combined technology can reduce oil saturation in low-permeability layers to 45.3% and improve recovery by 30.2% compared to water flooding. Field trials proved to be completely effective, with a cumulative oil increase of over 23,200 cubic meters and a 12% reduction in water cut per well. This deep profile control technology offers significant water cut reduction and enhanced oil recovery. It can provide technical support for efficient water control and profile management in similar reservoirs.



Academic Editors: Junjian Zhang and Zhenzhi Wang

Received: 15 November 2024

Revised: 14 January 2025

Accepted: 16 January 2025

Published: 20 January 2025

Citation: Zheng, X.; Wang, Y.; Lei, Y.; Zhang, D.; Bao, W.; Huang, S. Research and Application of Deep Profile Control Technology in Narrow Fluvial Sand Bodies. *Processes* **2025**, *13*, 289. <https://doi.org/10.3390/pr13010289>

Copyright: © 2025 by the authors. Licensee MDPI, Basel, Switzerland. This article is an open access article distributed under the terms and conditions of the Creative Commons Attribution (CC BY) license (<https://creativecommons.org/licenses/by/4.0/>).

Keywords: narrow channel sand bodies; horizontal wells; injection–production well network; deep profile control and flooding; enhanced oil recovery

1. Introduction

With the ever-rising global demand for energy, finding new energy resources and increasing the efficiency of production from current sources are essential. This includes both emerging energy resources such as unconventional hydrocarbon sources, hydrates, and hydrogen gas, as well as increased efficiency of production and resource recovery, especially enhanced oil recovery [1–9]. Here, we describe recent innovations and successes in enhanced oil recovery in the Bohai Oilfield. The Bohai Oilfield is the largest offshore oilfield in China. The Bohai Sea covers an area of approximately 73,000 square kilometers, of which the explorable mining area is about 43,000 square kilometers, with a total resource of around 12 billion cubic meters. In 1967, China’s first offshore exploration well, “Haiyi Well”, marked the beginning of the production history of Bohai Oilfield. In 2021, the crude oil production of Bohai Oilfield reached 30,132 million tons, becoming the largest crude oil production base in China.

Due to the lifespan limitations of offshore platforms, the Bohai Oilfield typically adopts a high-intensity injection and production process. For narrow channel sand bodies,

horizontal wells provide a large flow area and high sweeping intensity for injection and production, but the single direction flow leads to a rapid increase in water cut. This results in increasingly significant conflicts in planar injection–production, progressively complex channel development, and the gradual migration of residual oil to deeper zones. These factors severely restrict the effectiveness of water flooding development [10–14].

In recent years, to meet the complex profile modification and displacement treatment requirements in deep reservoirs, petroleum researchers have conducted extensive studies. Junjian Li et al. conducted core flooding experiments to investigate the performance of nanosphere suspensions, poly(ethylene glycol) (PEG) single-phase gel particles, and crosslinked bulk gel swelling particles (CBG-SPs). The results showed that 100 nm nanospheres exhibit excellent in-depth profile control performance in low-permeability reservoirs, especially in dominant channels with permeabilities ranging from 50 to 100 mD [15]. Bozhao Xu et al. developed novel wet-phase modified expandable graphite (WMEG) particles for in-depth profile control in carbonate reservoirs [16]. Considering the pore structures of different reservoirs and the microsphere sizes used for oil displacement, Hongfu Shi carried out detailed pilot test designs aimed at minimizing slug size while maximizing net revenue [17]. Guang Zhao et al. used phenolic resin crosslinked NPAM gel as an in-depth profile control agent for water production control. This structure enhances the long-term stability of NPAM gel systems, effectively seals high-permeability zones, and improves formation profile control [18]. Bao Cao et al. found that using a composite gel system for profile modification and water shutoff operations can effectively treat channeled layers and improve the macroscopic sweep efficiency of oil displacement agents. In deep displacement systems using surfactant/microsphere composites, the microspheres can achieve micro-fluid diversion by blocking swept pores, while the surfactant solution can enter unswept pores to displace residual oil [19]. The aforementioned studies are primarily based on homogeneous physical simulation conditions. These studies demonstrate the advantages and characteristics of various profile control and flooding systems [20]. However, there is limited research on the effectiveness of plugging using different profile control oil displacement technologies under narrow fluvial horizontal well patterns [21,22].

Based on the actual issues and application scenarios of the Bohai narrow fluvial oilfields, this paper investigates the plugging capability and enhanced oil recovery effects of a heterogeneous in-depth profile control technology, including emulsion polymer gel profile control and self-assembling particle flooding. The investigation was conducted through microscopic analysis and physical simulation experiments. Additionally, field application results were analyzed to provide technical support for efficient profile control in offshore oilfields with similar reservoir characteristics.

2. Research Background

2.1. The Introduction of Narrow Fluvial Channel Sand

The Ming Lower Section A sand body of the Bohai C Oilfield is a typical narrow channel reservoir [23]. It mainly develops three stages of channels from bottom to top, which are stacked or separated at different stages in profile, presenting a narrow fluvial channel sedimentation pattern [24]. The sand bodies are arranged in an interbedding pattern, with sand bodies trending northwest and northeast. The crude oil viscosity in the Ming Lower Section A sand body is 90 mPa·s, and the reservoir temperature is 84 °C. This sand body is primarily developed through a horizontal well injection–production network [25]. From November 2005 to October 2017, the field was developed using a natural energy depletion method. After that, the first water injection well was put into operation. Currently, the sand body has 12 oil production wells and 4 water injection wells, with a geological reserve recovery degree of 20.4%. During water injection development,

due to the heterogeneity of the reservoir and the high injection intensity of horizontal wells, predominant pathways between wells have developed, leading to severe water channeling, which has exacerbated planar conflicts, as shown in Figure 1.

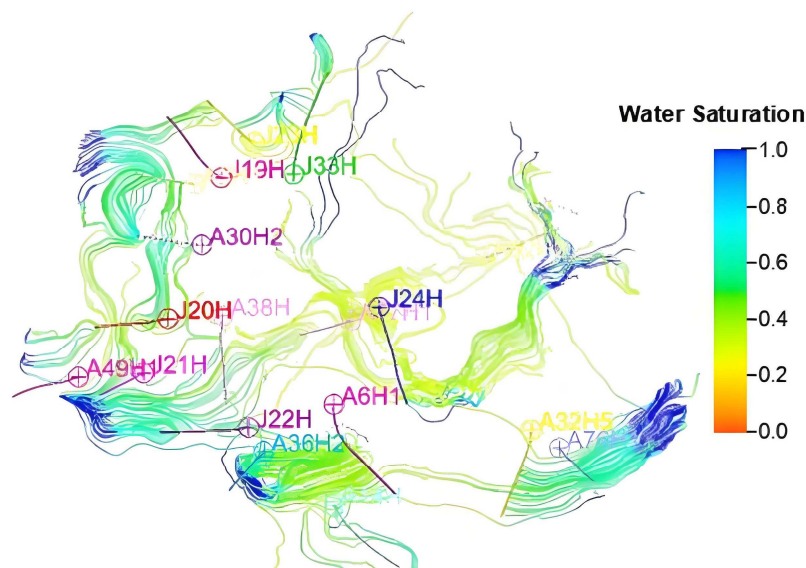


Figure 1. Planar flow pattern of the Ming Lower Section A sand body in Bohai C Oilfield.

2.2. Identification of Dominant Flow Channels in Narrow Fluvial Channel Sand Bodies

The Ming Lower Section A sand body of the Bohai C Oilfield develops typical low-bend meandering river deposits, with sand bodies forming narrow belt-like structures [26]. The reservoir connectivity is relatively good along the direction of the river channel. In plain view, the intersections of different belts represent the communication zones between channels. Longitudinally, multi-stage channels are often stacked and cut, forming complex fluid migration pathways [27]. Both the planar and longitudinal distributions of the sand body exhibit strong heterogeneity [28]. The vertical permeability contrast of the sand body ranges from 3 to 10, and the horizontal wells are deployed perpendicular to the river channels [29]. Along the horizontal wellbore, the permeability contrast ranges from 2 to 5. After water injection development, the injection volume along the horizontal well is uneven, and the breakthrough of high-permeability layers in the vertical direction is prominent. This leads to ineffective water injection circulation between oil and water wells.

The distribution of channeling pathways in a planar spindle shape can be calculated using numerical methods to determine the injection flowline distribution. Based on the spindle-shaped distribution on the injection plane (Figure 2), a monotonic correlation exists between multiple water injections, water saturation, and multiple permeability variations. This leads to the proposal of an “equivalent diffusion coefficient” based on “saturation difference”. This concept equates the effect of expanding the reservoir permeability on the axial and lateral distribution of injected water to the impact of mass transfer diffusion, thus describing the distribution of injected fluids between injection and production wells.

For the injection–production well profile model shown in Figure 3, it is assumed that the water saturation along the Z-axis direction in the channeled flow path is uniform, and that the injected water primarily moves along the “high-permeability channeled flow layer”. Based on the one-dimensional mass transfer diffusion equation, the effect of dilution caused by the distribution of injected water in non-channel flow paths on the water cut change at the production end is considered. The dilution factor α is defined as follows [30]:

$$\alpha = \frac{\frac{T_k \times b}{\mu_w}}{\frac{T_k \times b}{\mu_w} + \frac{1 \times (1-b)}{\mu_o}} \tag{1}$$

where T_k is the breakthrough coefficient of permeability in the channeled flow path, b is the proportion of the channeled flow path to the total reservoir thickness, μ_w is the water phase viscosity, and μ_o is the oil phase viscosity. The production end water cut can be expressed as follows:

$$f_w = \frac{1}{2} \alpha \cdot \operatorname{erfc}\left(\frac{x - ut'}{2\sqrt{Dt'}}\right) + f_{w0} \tag{2}$$

where D is the equivalent diffusivity, u is the injection rate, f_{w0} is the water cut corresponding to the initial oil saturation of the reservoir, t' is the correction time, and $\operatorname{erfc}(x)$ is the Gaussian error function.

$$t' = (1 - S_{wc})t \tag{3}$$

where S_{wc} is the irreducible water saturation.

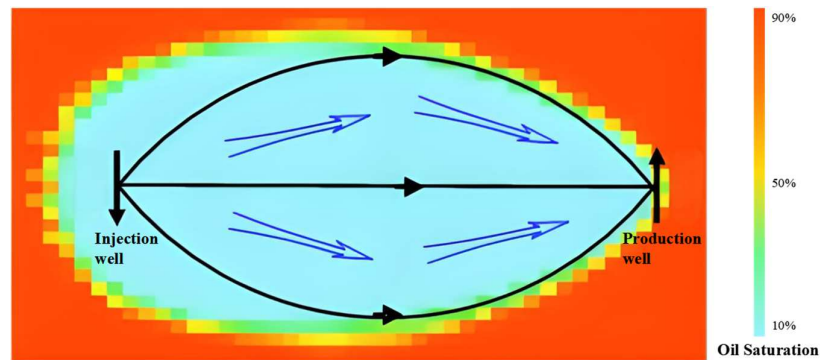


Figure 2. Characteristics of water injection distribution.



Figure 3. Physical model of injection-production well profile in high-permeability reservoir.

Using the above mathematical model, a method for quantifying the identification of dominant flow channels under the integration of dynamic and static big data constraints was established. This method combines static basic data, including the permeability of target well groups, injection–production well distance, formation thickness, and porosity. It also incorporates dynamic production data, such as production time, daily liquid production, and daily oil production. By fitting historical measured water cut curves, the parameters of high-permeability flow channels between injection and production wells are calculated inversely. The method was applied to analyze the Ming Lower Section A sand body. The results indicate the presence of water breakthrough in several high-permeability strips: (1) between J19H, A03H1, and J23H; (2) between A30H2, A3H1, and J20H; (3) between J21H, J20H, and J22H; and (4) between A36H2, J22H, and A06H1. Overall, the

connectivity of the western sand body was good, and the breakthrough velocity inversion results are shown in Figure 4.

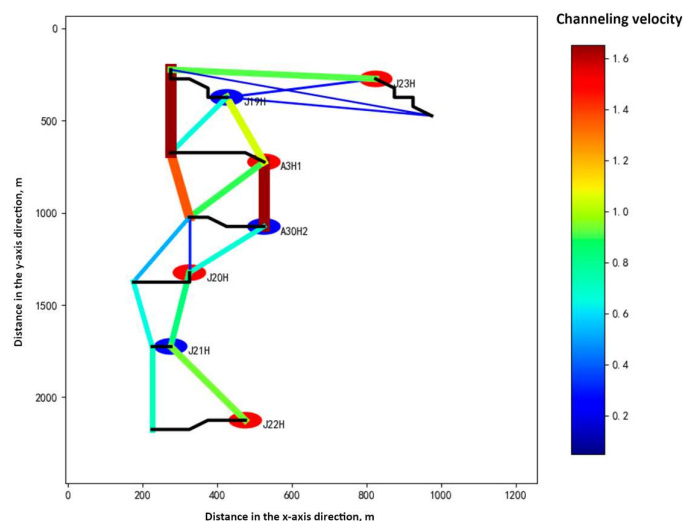


Figure 4. Distribution map of strong channeling between wells in the Ming Lower Section A sand body of Bohai C Oilfield.

In summary, the main issues in the development of the Ming Lower Section A sand body of the Bohai C Oilfield include the following. Firstly, there is local high-permeability strip channeling in the horizontal section at the oil well end. In some wells, the water cut increases sharply in the planar view, which urgently requires enhanced oil recovery and water control measures. Secondly, there is a water breakthrough issue at the water injection well end, and significant differences in liquid production and water cut are observed in the planar view. Flow field regulation has a positive effect on enhancing the production capacity of low liquid production and low water cut wells. Given that water injection profile control can expand the volume of injected water, suppress water breakthrough, and be an effective technical measure to improve development effects, the profile control measures for water injection wells have effectively slowed down the natural decline of the oilfield and significantly stabilized oil and water control. Therefore, it is necessary to implement deep combination profile control and flooding experiments on horizontal wells to further improve the water drive development effect.

2.3. Research on In-Depth Profile Control and Flooding Technology for Horizontal Well Injection–Production Networks

Narrow channel reservoirs, influenced by channel width, often adopt a “linear” horizontal well network along the center of the channel, as shown in Figure 5. This “linear” horizontal well network, combined with strong heterogeneity in the horizontal section, is characterized by a single displacement direction and high injection–production intensity, resulting in complex residual oil distribution patterns. To clarify the mobilization characteristics of residual oil under horizontal well injection–production network conditions and to explore the impact of different profile control and flooding combinations on oil enhancement, this study utilized commonly used polymer latex gels, self-aggregating particles, and flooding systems in offshore oilfields. Laboratory performance evaluations were performed, and a heterogeneous flat core model was used to simulate the “linear” horizontal well network. Along with resistivity data from cores, the analysis of residual oil mobilization and the study of mechanism effects were conducted, providing valuable insights for field applications in similar reservoirs.

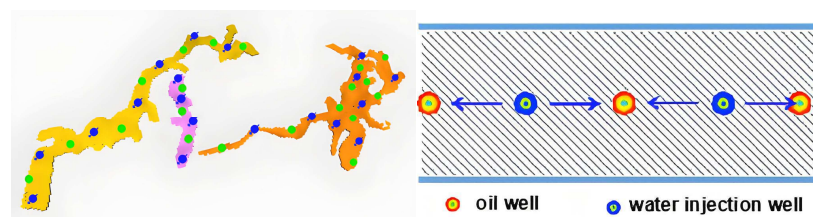


Figure 5. “Linear” well network and schematic diagram of narrow channel sand bodies.

3. Materials and Methods

3.1. Materials

The experimental agents include an emulsion polymer gel profile control agent, a self-aggregating particle flooding agent, and an oil displacement agent (CNOOC, Tianjin, China). The emulsion polymer gel profile control agent is a polymer system prepared by inverse emulsion polymerization, which features fast dissolution, low initial viscosity, and no need for maturation. In the presence of a phenolic crosslinking agent, it can form a gel profile control system. The self-aggregating particle flooding agent consists of water-based particles prepared by dispersion polymerization, which offer better dispersion and ease of injection compared to traditional microspheres. These particles can self-aggregate through electrostatic forces, enhancing deep profile control and blocking effects. The oil displacement agent primarily comprises emulsifying viscosity-reducing surfactants.

The experimental oil is a mixture of kerosene and degassed crude oil in a fixed proportion and has a viscosity of 70 mPa·s at reservoir temperature. The experimental water is formation-simulated water, with water quality analysis shown in Table 1. Based on the actual static and dynamic geological data of the sand body, the experimental core was designed as a heterogeneous flat core made of quartz sand bonded with epoxy resin (core permeability: $10,000/5000/2000 \times 10^{-3} \mu\text{m}^2$). The core dimensions were 32 cm \times 32 cm \times 6 cm (length \times width \times height). The electrode substrate material was pure copper, with a surface chemically plated with a nickel–phosphorus alloy layer. The electrodes were evenly distributed throughout the core with a spacing of 2 cm and a depth of 3 cm. Electrodes were placed on the core surface to measure resistivity in different positions, enabling analysis of oil saturation. A schematic diagram of the core and the positions of the oil and water wells is shown in Figure 6a, and the core surface electrodes are shown in Figure 6b.

Table 1. Water quality composition.

Ion Composition and Concentration (mg·L ⁻¹)							Total (mg·L ⁻¹)
K ⁺ + Na ⁺	Ca ²⁺	Mg ²⁺	Cl ⁻	SO ₄ ²⁻	CO ₃ ²⁻	HCO ₃ ⁻	
2323.9	171.5	21.8	3 641.3	12.6	56.1	825.4	7052.7

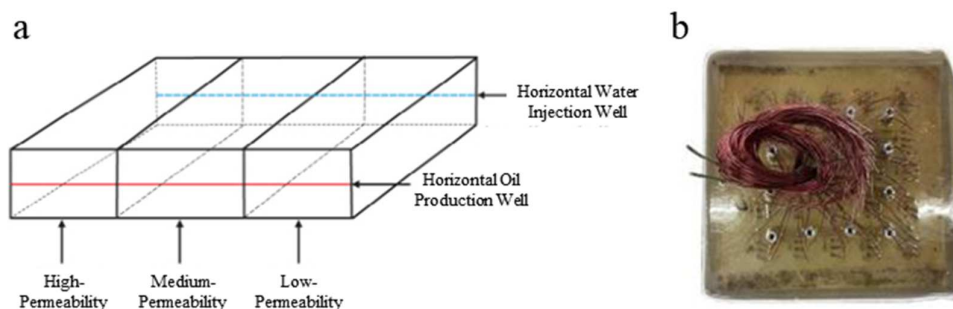


Figure 6. Core schematic diagram: (a) model schematic; (b) physical model image.

3.2. Methods

(1) System Performance Characterization

The performance of the polymer latex gel profile control agent was evaluated with a Brookfield viscometer (AMETEK Brookfield, Middleborough, MA, USA). The microscopic morphology of the gel profile control agent and the self-aggregating particle flooding agent was examined with a Quanta FEG450 (FEI Co., Hillsboro, OR, USA) field emission scanning electron microscope. The particle size distribution of the self-aggregating particle flooding agent was measured with a Malvern Zetasizer 3000HSA (Malvern Panalytical, Malvern, UK) particle size analyzer. The interfacial tension between the oil displacement agent and crude oil was tested with a TX-500C (Shanghai Zhongchen Digital Technology Equipment Co., Ltd., Shanghai China) spinning drop interfacial tensiometer.

(2) Evaluation of Oil Increment and Residual Oil Distribution

Scheme 1: Saturated oil + water flooding until the outlet water cut reaches 80% + 0.2 PV of self-aggregating particle flooding agent (0.3% concentration) + 0.1 PV of oil displacement agent (0.15% concentration) + water flooding until 95%.

Scheme 2: Saturated oil + water flooding until the outlet water cut reaches 80% + 0.05 PV of emulsion polymer gel profile control agent (0.6% polymer concentration + 0.5% crosslinker concentration, cured for 5 days) + 0.2 PV of self-aggregating particle flooding agent (0.3% concentration) + water flooding until 95%.

Scheme 3: Saturated oil + water flooding until the outlet water cut reaches 80% + 0.05 PV of emulsion polymer gel profile control agent (0.6% polymer concentration + 0.5% crosslinker concentration, cured for 5 days) + 0.2 PV of self-aggregating particle flooding agent (0.3% concentration) + 0.1 PV of high-efficiency oil displacement agent (0.15% concentration) + water flooding until 95%.

In the experiment, electrodes arranged on a flat core allowed for separate measurement of resistance values across different layers, enabling monitoring of the oil–water saturation distribution during displacement. The principle is based on the high resistivity of crude oil and the low resistivity of water, which allows differentiation between oil and water based on their resistivity values. To accurately determine changes in water saturation at each point, a calibration experiment was performed in advance to establish the relationship between resistance values and saturation. Oil and water were injected into the model at set ratios (19:1, 9:1, 4:1, 1:1, and 1:4). Resistance values were measured at different water saturation levels to obtain a correlation between resistance and saturation. During the water injection displacement process, the resistance of each layer in the flat model was measured using a resistance meter, and water saturation values were calculated using the fitted formula. A saturation map was then plotted to visually observe the oil–water movement.

4. Results and Discussion

4.1. System Performance Characterization

4.1.1. Gelation Performance of Emulsion Polymer Gel

At 65 °C, different concentrations of emulsion polymer and crosslinker were prepared to evaluate the viscosity changes in the system over time. The experimental results are shown in Figure 7. The initial viscosity of the polymer latex gel system is relatively low but gradually increases after aging for 5 days. With higher concentrations of emulsion polymer and crosslinker, the system viscosity increases more significantly over the same time intervals. After approximately 15–20 days, the viscosity of the gel system stabilizes, reaching a range of 25,000 to 30,000 mPa·s, indicating good delayed gelation performance and gel strength.

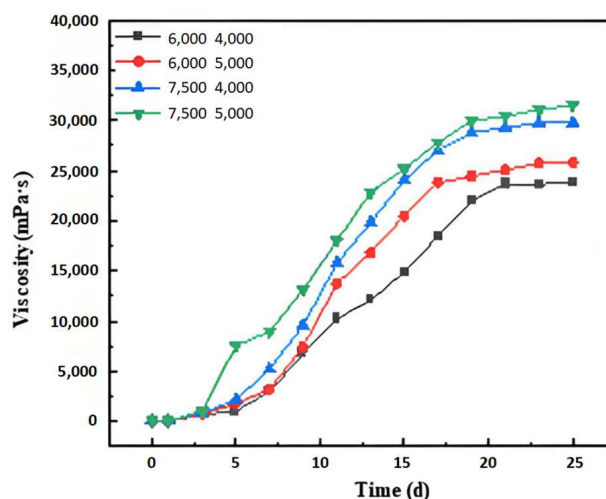


Figure 7. Gelation performance of emulsion polymer gel.

4.1.2. Microscopic Morphology of Emulsion Polymer

The microscopic morphology of the emulsion polymer and the emulsion polymer gel after gelation is shown in Figure 8. The emulsion polymer exhibits a milk-like microscopic morphology, with observable spherical structures of varying forms. After the addition of a crosslinker to induce gelation, the microscopic structure reveals a crosslinked network structure. Some spherical particles are still visible in certain areas, which are presumed to be polymer particles that did not fully participate in the crosslinking reaction.

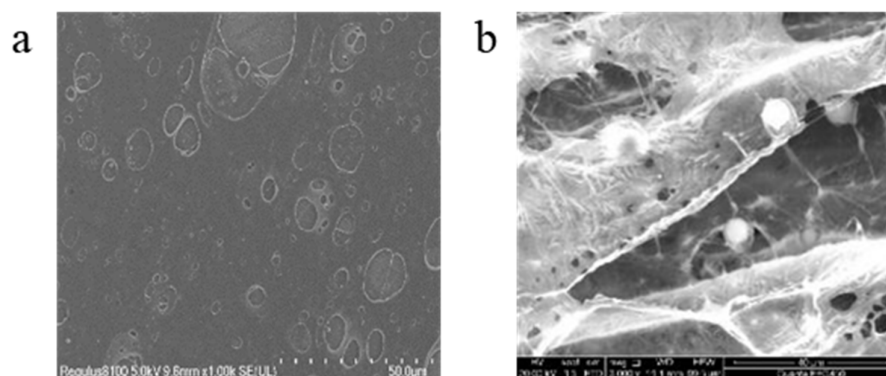


Figure 8. Microscopic morphology of emulsion polymer and gel. (a) Emulsion polymer (at 50 μm scale); (b) emulsion polymer gel (at 40 μm scale).

4.1.3. Particle Size Testing of Self-Aggregating Particles

Different concentrations of self-aggregating particles ($500 \text{ mg}\cdot\text{L}^{-1}$, $1000 \text{ mg}\cdot\text{L}^{-1}$, $2000 \text{ mg}\cdot\text{L}^{-1}$, $3000 \text{ mg}\cdot\text{L}^{-1}$) were added to simulated water to measure the change in average particle size over aging time, with results shown in Figure 9. The initial particle size of the self-aggregating particles is around 500 nm. As aging time increases, the particle size first rises sharply, then increases more gradually, reaching equilibrium at around 20 days. The higher the concentration, the less time is required to reach equilibrium size.

4.1.4. Microscopic Morphology of Self-Aggregating Particles

The microscopic morphology of self-aggregating particles is shown in Figure 10. It can be observed that the self-aggregating particles have a regular spherical shape. The hydrophilic groups on their surface control the rate and amount of hydration layer formation, which enables the particles to self-aggregate through ionic bonding.

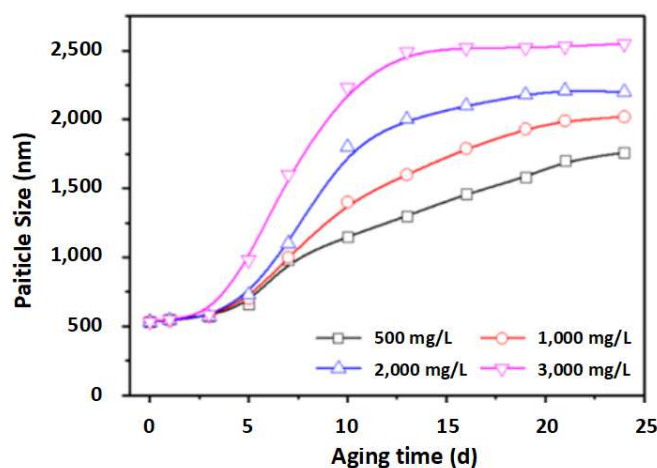


Figure 9. Relationship between particle size and aging time for samples of different concentrations.

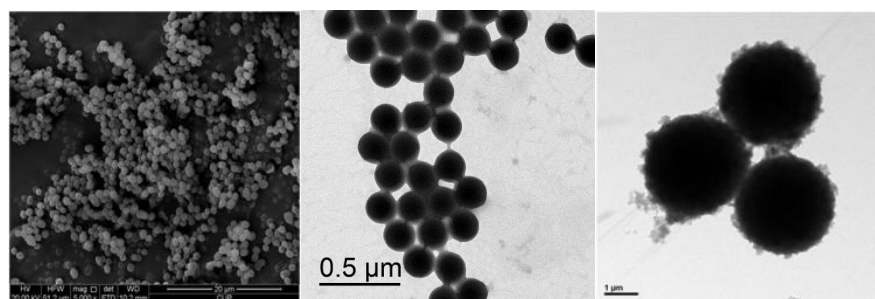


Figure 10. Microscopic morphology of self-aggregating particles.

4.2. Performance Evaluation

4.2.1. Interfacial Tension of Oil Displacement Agent

Solutions of the oil displacement agent were prepared at different concentrations ($500 \text{ mg}\cdot\text{L}^{-1}$, $1000 \text{ mg}\cdot\text{L}^{-1}$, $1500 \text{ mg}\cdot\text{L}^{-1}$, and $2000 \text{ mg}\cdot\text{L}^{-1}$), and the interfacial tension with crude oil was measured, as shown in Table 2. As the concentration of the high-efficiency oil displacement agent increases, the interfacial tension with crude oil decreases. Considering cost-effectiveness, a concentration of $1500 \text{ mg}\cdot\text{L}^{-1}$ is recommended.

Table 2. Interfacial tension test results.

	Concentration (mg/L)			
	500	1000	1500	2000
Interfacial Tension ($\text{mN}\cdot\text{m}^{-1}$)	0.96×10^{-1}	1.58×10^{-1}	8.42×10^{-2}	6.13×10^{-2}

4.2.2. Evaluation of Oil Increment Effect and Residual Oil Distribution

(1) Analysis of Enhanced Oil Recovery Increment

The experimental results for enhanced oil recovery are shown in Table 3. It can be seen that, compared to the water flooding stage, the injection of polymer latex gel does not significantly increase the stage recovery factor. This is partly due to the small slug size of the emulsion polymer gel injection (0.05 PV) and its initially low viscosity, which mainly allows it to enter the high-permeability channels, resulting in limited displacement of residual oil. Comparing the stage recovery factors of the self-aggregating particle flooding agent across the three schemes reveals that the emulsion polymer gel significantly enhances the effect of the self-aggregating particle flooding. This is because the emulsion polymer

gel effectively blocks the high-permeability zones, directing the self-aggregating particles into medium- and low-permeability zones. This further regulates secondary flow channels and expands the sweep volume. The recovery factor during the flooding stage reaches approximately 42.6%. Additionally, this process facilitates sufficient contact between the oil displacement agent and residual oil, enhancing the oil-washing effect, which ultimately results in a substantial increase in the final water flooding recovery factor to 57.1%, a 30.2% increase compared to the end of the water flooding stage.

Table 3. Recovery rate experimental data.

Scheme	Oil Saturation (%)	Water Flooding	Stage Recovery Factor (%)			Recovery Factor (%)	
			Gel	Self-Aggregating Particles	Oil Displacement Agent	Final	Increment
1	70.7	26.2	/	30.0	35.6	46.0	19.8
2	70.2	26.7	28.6	42.7	/	48.5	21.8
3	70.6	26.9	28.2	42.6	49.1	57.1	30.2

(2) Analysis of Oil Saturation Distribution

The average residual oil saturation for each layer at the end of each displacement stage is shown in Tables 4–6. The overall oil saturation distribution is shown in Figures 11–13. During water flooding, when the outlet water cut reaches 80%, the injected water primarily flows through the high-permeability zones with high sweep efficiency. The oil saturation in high-permeability layers decreases significantly to 36.3–37.2%, which indicates good water flooding performance in these layers.

Table 4. Average residual oil saturation at each stage (Scheme 1).

Injection Stage	Oil Saturation (%)		
	High Permeability	Medium Permeability	Low Permeability
End of Water Flooding with Outlet Water Cut Reaching 80%	59.4	46.1	37.2
End of Self-Aggregating Particle Injection Stage	59.1	41.8	34.7
End of Oil Displacement Agent Injection Stage	54.6	38.7	33.6
End of Subsequent Water Flooding	50.7	37.6	31.9

Table 5. Average residual oil saturation at each stage (Scheme 2).

Injection Stage	Oil Saturation (%)		
	High Permeability	Medium Permeability	Low Permeability
End of Water Flooding with Outlet Water Cut Reaching 80%	58.5	45.2	36.3
End of Emulsion Polymer Gel Injection Stage	58.2	44.9	34.1
End of Self-Aggregating Particle Injection Stage	52.7	39.9	32.6
End of Subsequent Water Flooding	49.3	38.1	31.5

Table 6. Average residual oil saturation at each stage (Scheme 3).

Injection Stage	Oil Saturation (%)		
	High Permeability	Medium Permeability	Low Permeability
End of Water Flooding with Outlet Water Cut Reaching 80%	58.7	45.6	36.8
End of Emulsion Polymer Gel Injection Stage	58.4	45.4	34.1
End of Self-Aggregating Particle Injection Stage	53.8	40.2	33.0
End of Oil Displacement Agent Injection Stage	48.1	36.3	32.2
End of Subsequent Water Flooding	45.3	33.6	27.2

Compared to the injection of polymer gel, self-aggregating particles improve displacement between medium-high- and medium-permeability zones to some extent, reducing oil saturation in the medium-permeability layer after water flooding. This effect is attributed

to the relatively larger slug size of self-aggregating particles, which enables partial plugging at the entrance of high-permeability layers, thereby allowing subsequent fluids to displace the medium-permeability layer. However, the final oil saturation distribution indicates that the blocking effect of self-aggregating particles is limited, and their performance in displacing oil from low-permeability layers is suboptimal.

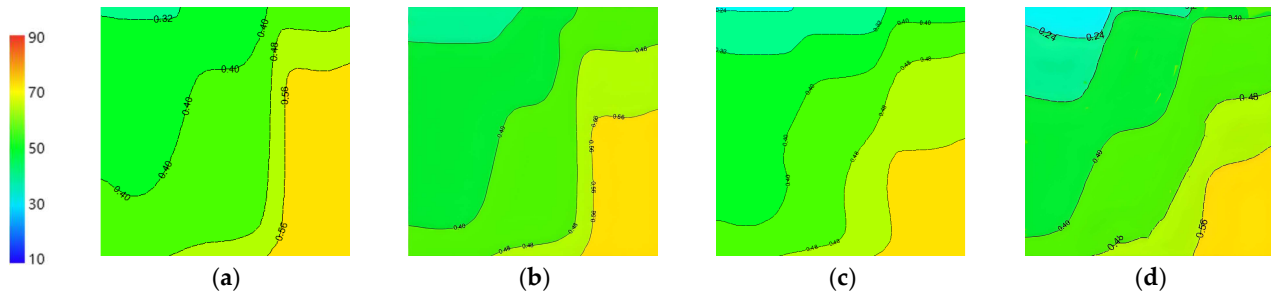


Figure 11. Oil saturation distribution at different stages in Scheme 2: (a) water flooding, (b) self-aggregating particles, (c) oil displacement agent, (d) subsequent water flooding.

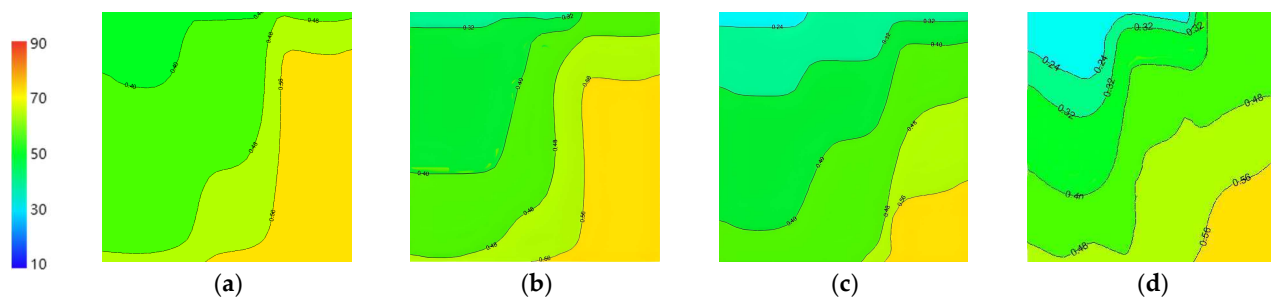


Figure 12. Oil saturation distribution at different stages in Scheme 2: (a) water flooding, (b) emulsion polymer gel, (c) self-aggregating particles, (d) subsequent water flooding.

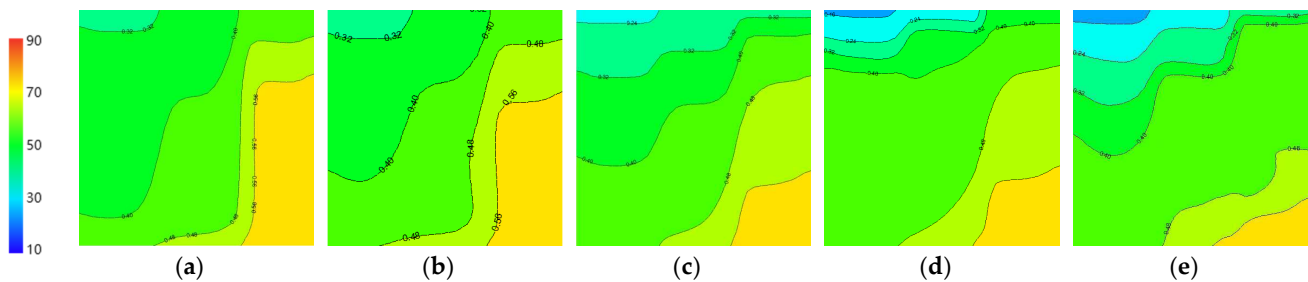


Figure 13. Oil saturation distribution at different stages in Scheme 3: (a) water flooding, (b) emulsion polymer gel, (c) self-aggregating particles, (d) oil displacement agent, (e) subsequent water flooding.

Comparing Schemes 2 and 3, the gel mainly enters the high-permeability layer during injection, resulting in minimal sweep effect during injection. This is due to the low initial viscosity of the system, which allows it to flow along water pathways while preserving the integrity of the medium- and low-permeability layers. After gelation, the flow resistance in the high-permeability layer increases, forcing subsequent fluids to redirect into medium- and low-permeability layers, thus reducing oil saturation in these layers and improving overall displacement efficiency.

Overall, the combined displacement technology (Scheme 3) achieves selective and staged blocking in heterogeneous sections of the horizontal well. The polymer gel system effectively seals high-permeability channels without damaging medium- and low-permeability layers, allowing self-aggregating particles to adjust secondary water channels.

This facilitates full contact between the subsequent oil displacement agent, water, and residual oil, enhancing overall water flooding efficiency.

5. Field Application

To fully leverage the synergistic effects of each well intervention, the overall flooding control adheres to a strategy of single-round integrated design, phased implementation, and deep potential tapping. Guided by comprehensive profile control and flooding design, high water channeling wells are prioritized for polymer gel profile control to seal high-permeability layers. This is followed by self-aggregating particle flooding to expand the sweep volume from targeted areas to a wider region. Finally, an oil displacement agent system is injected to uniformly displace the residual oil in the reservoir, thereby enhancing the overall development effect.

In field applications, Bohai C Oilfield implemented this heterogeneous deep combination flooding system for wells with severe water channeling, such as well groups A30H2, J19H, and J21H. For the A30H2 well group, the total injection volume of the deep flooding system was 34,465 cubic meters, resulting in an incremental oil production of 7514 cubic meters. The J19H well group had a total injection volume of 41,494 cubic meters with an oil increase of 5634 cubic meters, while J21H reached 30,313 cubic meters of injected volume, with an incremental oil production of 10,139 cubic meters. To date, the sand body’s combined flooding operations have shown significant water reduction and oil enhancement, with a cumulative oil increase exceeding 23,200 cubic meters and an input–output ratio of over 1:3, as shown in Table 7 and Figure 14.

Table 7. Summary of comprehensive flooding control implementation for the Section A Sand Body in the Mingxia Formation.

Well Group	Channeling Volume/m ³	Injection Volume (m ³)		Profile Control Slug Injection Parameters		Flooding Control Slug Injection Parameters		Production Increase/m ³	Input–Output Ratio
		Total	Profile Control	Pressure Increase/MPa	Fill Factor/%	Pressure Increase/MPa	Fill Factor/%		
A30H2	57,389	34,465	6178	28,287	6.8~7.3	30.9	4.9~6.8	41.9	1:3.6
J19H	48,403	41,494	6917	34,577	4.0~5.6	43.4	7.4~9.0	60.3	1:3.1
J21H	57,153	30,313	5500	19,827	4.4~7.0	21.7	6.9~9.0	46.2	1:3.9

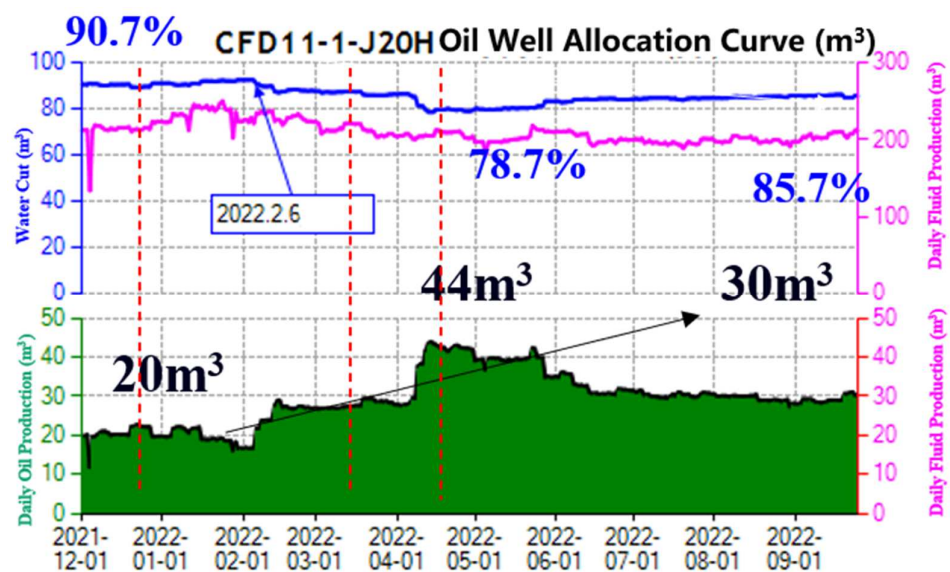


Figure 14. J20H well production curve.

Taking the A30H2 well group as an example, the effective well J20H, after injecting the gel and self-aggregating particle combination flooding system, achieved a peak daily oil increase of 24 cubic meters and a maximum water cut reduction of 12%. The duration of effectiveness exceeded 12 months, demonstrating significant oil enhancement, as illustrated in the figure.

The next step will be to conduct research and experiments on combined deep profile control technology under different reservoir conditions; optimize injection timing, injection dosage, and injection concentration; and expand the adaptability of the technology. This technology, with its advantages of “effective injection, secure blockage, deep penetration, and thorough sweeping”, offers significant application potential. It provides technical support for stable oil production, water control, and efficient flooding management in similar reservoirs.

6. Conclusions

- (1) To quantitatively describe the development of dominant channels and water breakthrough in injection–production well groups of narrow channel sand bodies, a quantitative identification method based on dynamic–static big data integration constraints for dominant channels was established. This method quantifies the flow intensity between water injection wells and affected oil wells, providing a foundation for the design of deep driving adjustment schemes for subsequent well groups.
- (2) With the Ming Lower Section A sand body of Bohai C Oilfield as the experimental target and microscopic analysis and physical simulation as the technical means, a heterogeneous flat core model was used to simulate horizontal well injection–production patterns. Combined with core resistivity test data, residual oil distribution analysis and oil increase effect evaluation were conducted. Deep combined driving adjustment technology, primarily utilizing emulsion polymer gel profile control and self-assembling particle driving adjustment, was developed. Experimental results show that the combined driving adjustment technology can achieve zoned and staged plugging, ultimately reducing the oil saturation of low-permeability layers to 45.3%, with an overall recovery rate increased by 30.2% compared to that of water flooding.
- (3) In the Bohai C Oilfield, a heterogeneous deep combined driving adjustment system mainly based on emulsion polymer gel profile control and self-assembling particle driving adjustment was adopted for the Ming Lower Section A sand body. A pilot test for water injection well group driving adjustment was conducted on three wells. After applying the driving adjustment measures to the sand body, significant improvements in water cut reduction and oil production increase were achieved. Specifically, a cumulative oil increase of over 23,200 m³ was achieved, and the maximum water cut reduction per well reached 12%. This technology has technical advantages including easy injection, effective plugging, deep driving, and clean washing. It has significant application potential and provides technical support for stable oil production, water control, and efficient driving adjustment in similar reservoirs.

Author Contributions: Methodology, X.Z. and S.H.; Validation, Y.L.; Investigation, Y.W.; Resources, D.Z.; Data curation, W.B. All authors have read and agreed to the published version of the manuscript.

Funding: This research was funded by the 14th Five-Year Plan of the Major Science and Technology Project in CNOOC Ltd. (project number: KJGG2021-0501).

Data Availability Statement: The original contributions presented in this study are included in the article. Further inquiries can be directed to the corresponding author.

Conflicts of Interest: Authors Xu Zheng, Yu Wang, Yuan Lei, Dong Zhang and Wenbo Bao were employed by Tianjin Branch of CNOOC Ltd. The remaining author declares that the research was conducted in the absence of any commercial or financial relationships that could be construed as a potential conflict of interest. The Tianjin Branch of CNOOC Ltd. had no role in the design of the study; in the collection, analyses, or interpretation of data; in the writing of the manuscript, or in the decision to publish the results.

References

1. Wolfram, C.; Shelef, O.; Gertler, P. How will energy demand develop in the developing world? *J. Econ. Perspect.* **2012**, *26*, 119–138. [[CrossRef](#)]
2. Shove, E.; Walker, G. What is energy for? Social practice and energy demand. *Theory Cult. Soc.* **2014**, *31*, 41–58. [[CrossRef](#)]
3. Mazloomi, K.; Gomes, C. Hydrogen as an energy carrier: Prospects and challenges. *Renew. Sustain. Energy Rev.* **2012**, *16*, 3024–3033. [[CrossRef](#)]
4. Abe, J.O.; Popoola, A.P.I.; Ajenifuja, E.; Popoola, O.M. Hydrogen energy, economy and storage: Review and recommendation. *Int. J. Hydrog. Energy* **2019**, *44*, 15072–15086. [[CrossRef](#)]
5. Burton, Z.; Kroeger, K.F.; Hosford Scheirer, A.; Seol, Y.; Burgreen-Chan, B.; Graham, S.A. Tectonic uplift destabilizes subsea gas hydrate: A model example from Hikurangi margin, New Zealand. *Geophys. Res. Lett.* **2020**, *47*, e2020GL087150. [[CrossRef](#)]
6. Burton, Z.F.M.; Dafov, L.N. Testing the sediment organic contents required for biogenic gas hydrate formation: Insights from synthetic 3-D basin and hydrocarbon system modelling. *Fuels* **2022**, *3*, 555–562. [[CrossRef](#)]
7. Burton, Z.F.M.; Dafov, L.N. Salt Diapir-Driven Recycling of Gas Hydrate. *Geochem. Geophys. Geosyst.* **2023**, *24*, e2022GC010704. [[CrossRef](#)]
8. Alvarado, V.; Manrique, E. Enhanced oil recovery: An update review. *Energies* **2010**, *3*, 1529–1575. [[CrossRef](#)]
9. Lake, L.W.; Johns, R.; Rossen, B.; Pope, G.A. *Fundamentals of Enhanced Oil Recovery*; Society of Petroleum Engineers: Richardson, TX, USA, 2014.
10. Xue, D.D.; Zheng, C.F.; Liu, Z.M.; Peng, J.Y.; Shen, Q. Enhanced oil recovery through balanced production techniques in horizontal wells of Bohai A Oilfield. *Acadlore Trans. Geosci.* **2024**, *3*, 13–23. [[CrossRef](#)]
11. Zhao, X.; Wang, C.; Wang, Q.; Tan, J.; Yang, W. A case of multi-stage fracturing horizontal well used in BZ oilfield in Bohai bay low-permeability oilfield development. *J. Geosci. Environ. Prot.* **2020**, *8*, 147–154. [[CrossRef](#)]
12. Høimyr, Ø.; Kleppe, A.; Nystuen, J.P. Effects of heterogeneities in a braided stream channel sandbody on the simulation of oil recovery: A case study from the Lower Jurassic Statfjord Formation, Snorre Field, North Sea. *Geol. Soc. Lond. Spec. Publ.* **1993**, *69*, 105–134. [[CrossRef](#)]
13. Willis, B.J.; Sech, R.P. Quantifying impacts of fluvial intra-channel-belt heterogeneity on reservoir behaviour. In *Fluvial Meanders and Their Sedimentary Products in the Rock Record*; Wiley: Hoboken, NJ, USA, 2018; pp. 543–572.
14. Deveugle, P.E.K.; Jackson, M.D.; Hampson, G.J.; Farrell, M.E.; Sprague, A.R.; Stewart, J.; Calvert, C.S. Characterization of stratigraphic architecture and its impact on fluid flow in a fluvial-dominated deltaic reservoir analog: Upper Cretaceous Ferron Sandstone Member, Utah. *AAPG Bull.* **2011**, *95*, 693–727. [[CrossRef](#)]
15. Li, J.; Wang, Z.; Yang, H.; Yang, H.; Wu, T.; Wu, H.; Wang, H.; Yu, F.; Jiang, H. Compatibility evaluation of in-depth profile control agents in dominant channels of low-permeability reservoirs. *J. Pet. Sci. Eng.* **2020**, *194*, 107529. [[CrossRef](#)]
16. Xu, B.Z.; Lv, D.F.; Zhou, D.Y.; Sun, N.; Lu, S.Y.; Dai, C.L.; Zhao, G.; Shi, M.M. Potential application of wet-phase modified expandable graphite particles as a novel in-depth profile control agent in carbonate reservoirs. *Pet. Sci.* **2024**, *21*, 4153–4164. [[CrossRef](#)]
17. Shi, H.; Ma, K.; Chen, C.; Shi, F.; Han, X. Pilot Test of Deep Profile Controlling and Sweep Improvement Based on Plugging Agent Location Optimization in Offshore Oilfield. In Proceedings of the Offshore Technology Conference Asia (OTC), Kuala Lumpur, Malaysia, 22–25 March 2022; p. D031S028R003.
18. Zhao, G.; Dai, C.; Chen, A.; Yan, Z.; Zhao, M. Experimental study and application of gels formed by nonionic polyacrylamide and phenolic resin for in-depth profile control. *J. Pet. Sci. Eng.* **2015**, *135*, 552–560. [[CrossRef](#)]
19. Cao, B.; Xie, K.; Lu, X.; Cao, W.; He, X.; Xiao, Z.; Zhang, Y.; Wang, X.; Su, C. Effect and mechanism of combined operation of profile modification and water shutoff with in-depth displacement in high-heterogeneity oil reservoirs. *Colloids Surf. A Physicochem. Eng. Asp.* **2021**, *631*, 127673. [[CrossRef](#)]
20. Meng, X.; Zhang, Y.; Xia, H.; Liu, Y.; Wang, W.; Lü, J.; Yin, Q. Study on Plugging and Displacement of Large-Size Advantage Channel in Bohai Oilfield. *J. Petrochem. Univ.* **2019**, *32*, 44.
21. Pan, G.; Zhan, C.; Liu, D. Weak-gel pro- file-control flooding to enhance oil recovery in offshore heavy-oil reservoir. *Spec. Oil Gas Reserv.* **2018**, *25*, 140–143.

22. Guo, T.; Su, Y. Current status and technical development direction in heavy oil reservoir development in Bohai oilfields. *China Offshore Oil Gas* **2013**, *25*, 26–30.
23. Xu, Z.; Kai, H.; Shen, C.; Luo, X.; He, B.; Kai, K.; Chen, Y.; He, X.; Lin, L.; Zhang, B. Architecture Characterization of Sandy Braided Fluvial reservoir: A Case study of P Oilfield (Neogene), Bohai Offshore, China. In Proceedings of the SPE Annual Technical Conference and Exhibition, SPE, Houston, TX, USA, 28–30 September 2015; p. D031S035R002.
24. Li, C.; Ma, F.; Wang, Y.; Zhang, D. Research on the prediction method for fluvial-phase sandbody connectivity based on big data analysis—A case study of Bohai A oilfield. *Artif. Intell. Geosci.* **2024**, *5*, 100095. [[CrossRef](#)]
25. Li, C.; Han, X.; Hu, Y.; Zhou, J.; Yan, T. Architecture of multiphase narrow-channel sand bodies of shallow water deltaic facies: A case study on BZ25-1S oilfield. *China Pet. Explor.* **2016**, *21*, 43.
26. Guo, T.; Yang, Q.; Huang, K.; Zhang, J. Techniques for high-efficient development of offshore fluvial oilfields. *Pet. Explor. Dev.* **2013**, *40*, 758–765. [[CrossRef](#)]
27. Hu, D.; Li, Z.; Wei, Z.; Duan, J.; Miao, Z.; Pan, L.; Li, C.; Duan, H. Major advancement in oil and gas exploration of Jurassic channel sandstone in Well Bazhong 1HF in northern Sichuan Basin and its significance. *Nat. Gas Ind. B* **2023**, *10*, 270–282. [[CrossRef](#)]
28. Zappa, G.; Bersezio, R.; Felletti, F.; Giudici, M. Modeling heterogeneity of gravel-sand, braided stream, alluvial aquifers at the facies scale. *J. Hydrol.* **2006**, *325*, 134–153. [[CrossRef](#)]
29. Chen, Q.; Liu, Y.; Feng, Z.; Hou, J.; Bao, L.; Liang, Z. The Architecture Characterization of Braided River Reservoirs in the Presence of Horizontal Wells—An Application in a Tight Gas Reservoir in the North Ordos Basin, China. *Energies* **2023**, *16*, 7092. [[CrossRef](#)]
30. Lei, X.L. Research on Reservoir Engineering Method for Identifying Advantageous Channels in Water Drive Reservoirs. Master's Thesis, China University of Petroleum, Beijing, China, 2018.

Disclaimer/Publisher's Note: The statements, opinions and data contained in all publications are solely those of the individual author(s) and contributor(s) and not of MDPI and/or the editor(s). MDPI and/or the editor(s) disclaim responsibility for any injury to people or property resulting from any ideas, methods, instructions or products referred to in the content.